APPLIED MICROBIAL AND CELL PHYSIOLOGY

Analysis of composition and structure of *Clostridium thermocellum* membranes from wild-type and ethanol-adapted strains

Michael D. Timmons · Barbara L. Knutson · Sue E. Nokes · Herbert J. Strobel · Bert C. Lynn

Abstract *Clostridium thermocellum is* a candidate organism for consolidated bioprocessing of lignocellulosic biomass into ethanol. However, commercial use is limited due to growth inhibition at modest ethanol concentrations. Recently, an ethanol-adapted strain of *C. thermocellum* was produced. Since ethanol adaptation in microorganisms has been linked to modification of membrane lipids, we tested the hypothesis that ethanol adaptation in *C. thermocellum* involves lipid modification by comparing the fatty acid composition and membrane anisotropy of wild-type and ethanol-adapted strains. Derivatization to fatty acid methyl esters provided quantitative lipid analysis. Compared to wild-type, the ethanol-adapted strain had a larger percentage of fatty acids with chain lengths >16:0 and showed a significant increase in the percentage of 16:0 plasmalogens. Structural identification of fatty acids was confirmed through mass spectral fragmentation patterns of picolinyl esters. Ethanol adaptation did not involve modification at sites of methyl branching or the unsaturation index. Comparison of steady-state fluorescence anisotropy experiments, in the absence and presence of ethanol, provided evidence for the effects of ethanol on membrane fluidity. In the presence of ethanol, both strains displayed increased fluidity by approximately 12%. These data support the model that ethanol adaptation was the result of fatty acid changes that increased membrane rigidity that counter-acted the fluidizing effect of ethanol.

M. D. Timmons · B. C. Lynn (✉)
Department of Chemistry, University of Kentucky,
Lexington, KY 40506-0046, USA
e-mail: bclynn2@uky.edu

B. L. Knutson
Department of Chemical and Materials Engineering,
University of Kentucky,
Lexington, KY 40506-0046, USA

S. E. Nokes
Department of Biosystems and Agricultural Engineering,
University of Kentucky,
Lexington, KY 40506-0046, USA

H. J. Strobel
Department of Animal and Food Sciences,
University of Kentucky,
Lexington, KY 40506-0046, USA

Introduction

Ethanol derived from fermentation of lignocellulosic biomass is a renewable alternative to petroleum-based transportation fuels. Virtually all bioethanol is currently produced from fermentation of corn starch by yeast, but these organisms are unable to directly degrade and ferment lignocellulosic feedstocks. Enzymatic, chemical, and physical pre-treatments are needed to saccharify structural carbohydrates, thus increasing the complexity and expense of the overall process. Consolidated bioprocessing by celluloytic bacteria has been proposed as an alternative technological platform for bioconversion of lignocellulose to ethanol (Lynd et al. 2002). There are many potential advantages to such a strategy, but a current limitation is the relatively low ethanol tolerance of cellulolytic bacteria. Most strains tolerate less than 1% (*w/v*) ethanol, while yeast tolerates concentrations that are at least tenfold greater (Alexandre et al. 1994b; Jones 1989).

Clostridium thermocellum is an anaerobic, thermophilic bacterium that metabolizes cellulose to ethanol and has been proposed for use in consolidated bioprocessing. Although the wild-type strain is sensitive to ethanol concentrations greater than 1% (w/v), certain ethanol-adapted cultures tolerate concentrations as high as 8% (w/v; Herrero and Gomez 1980; Rani et al. 1996; Williams et al. 2007). Herrero et al. (1982) described membrane lipid changes in an alcohol-adapted strain and showed an increased percentage of shorter (<C14) chain fatty acids and monounsaturated fatty acids when compared to the ethanol-sensitive wild type. In addition, *n*- and *anteiso*-branching was higher in the ethanol-adapted strain at the expense of *iso*-branching. However, there is little detailed information beyond this earlier work concerning the mechanism of ethanol adaptation in *C. thermocellum*.

Although there have been many investigations into solvent-induced membrane alterations in microorganisms (Ingram 1990; Jones 1989), much controversy remains. For instance, studies conducted on *Saccharomyces cerevisiae* found that the degree of monounsaturation and fatty acid chain length increased with ethanol exposure (Alexandre et al. 1994b). Additionally, experiments with *Kloeckera apiculata* showed an increase in 18:1 with a concurrent decrease in 16:1 when grown in the presence of ethanol, thus the degree of unsaturation remained unchanged (Alexandre et al. 1994b). However, bacterial studies with *Bacillus subtilis* and *Clostridium acetobutylicum* revealed an increase in long-chain fatty acids as a response to ethanol treatment (Weber and de Bont 1996). Such seeming discrepancies have led to different models for explaining ethanol adaptation, and these models usually speculate on physical properties such as membrane fluidity (Alexandre et al. 1994b; Weber and de Bont 1996).

The main objective of our work was to compare membrane composition of wild-type *C. thermocellum* with a recently isolated ethanol-adapted strain (Williams et al. 2007). Mass spectrometry was used to determine fatty acid structure and to quantify lipid abundance. In addition, functional aspects of the membrane were measured using steady-state fluorescence anisotropy. These experiments showed that ethanol adaptation was the result of fatty acid changes that increased membrane rigidity to counter act the fluidizing effect of ethanol.

Materials and methods

Reagents

Potassium *t*-butoxide (1.0 M) in tetrahydrofuran (THF), 3-hydroxymethyl pyridine, tridecanal, and hexane were purchased from Sigma (St. Louis, MO, USA). Methanol,

methylene chloride, and hydrochloric acid were obtained from Fisher (Pittsburg, PA, USA). Acetyl chloride was obtained from Fluka (Buchs, Switzerland). Sodium hydroxide, sodium bicarbonate, and potassium carbonate were purchased from J.T. Baker (Phillipsburg, NJ, USA). Ethyl ether was obtained from EMD (San Diego, CA, USA). Anthracene was purchased from Acros (Morris Plains, NJ, USA). Ethanol was purchased from Decon Laboratories (King of Prussia, PA, USA). GLC-411 lipid standard, 5,8,11,14-eicosatetraenoic acid (ARA), and 4,7,10,13,16,19-docosahexaenoic acid (DHA) were purchased from Nu-Chek Prep (Elysian, MN, USA), and 1,6-diphenyl-1,3,5-hexatriene (DPH) was purchased from Molecular Probes (Eugene, OR, USA).

Bacterial cultures and growth

C. thermocellum ATCC 27405 was obtained from the American Type Culture Collection. The wild-type (ethanol-sensitive) strain was adapted to ethanol as previously described (Williams et al. 2007). Cultures of wild-type and ethanol-adapted cells (13 L each) were grown in a basal medium that was previously described (Williams et al. 2007). Both strains were harvested during their respective growth phases, washed with 50 mM Tris (pH7.5), and stored at −80°C until analysis.

Saponification of fatty acids

Aliquots (15 mg cell dry weight) of *C. thermocellum* whole cells were washed three times with 1 mL portions of deionized H_2O, centrifuged (16,100×*g*, 5 min, 25°C), and the supernatants discarded. The cell pellets were placed at 0°C overnight and then vacuum-dried for 24 hat 25°C. The saponification methods were based on a previous description (Kurkiewicz et al. 2003). Sodium hydroxide (1 mL of 3 M) was added to the dried cells. The mixture was mixed and heated to 90°C for 1 h, cooled to room temperature, and 2 mL of 3.25 M HCl was added and reheated at 90°C for 10 min. After cooling to room temperature, the lipids were extracted three times with 1 mL portions of 1:1 (v/v) hexane/diethyl ether. The organic phases were combined and evaporated to dryness under a stream of N_2 at room temperature.

Fatty acid derivatization methods

Fatty acid methyl ester (FAME) procedures were adapted from previous studies (Lepage and Roy 1988). Methanol/acetyl chloride (50:1 (v/v), 5 mL total) was added to the extracted free fatty acids. The solution was mixed and heated at 60°C for 1 h. After heating, 3 mL of 6% K_2CO_3 was added, and the FAME products were extracted 1 mL

of hexane containing 0.1 mg anthracene (internal standard). Extracted material (1 μL) was used for GC/MS analysis.

Fatty acids were *trans*-esterified to picolinyl esters using an adapted method (Destaillats and Angers 2002). The hexane phase from the FAME procedure was evaporated to dryness under a stream of N_2 at room temperature, and 1 mL of methylene chloride was added to resolvate the methyl esters. In a separate vial, a mixture of 200 μL 3-hydroxymethylpyridine and 100 μL of 1.0 M potassium *tert*-butoxide in THF were allowed to react for 2 min. This mixture was then added to the FAME methylene chloride solution. The reaction was mixed and heated at 45°C for 1 h. After cooling to room temperature, 1 mL of 2.5% $NaHCO_3$ was added and the methylene chloride layer was removed. The organic layer was reduced to approximately one quarter original volume under a stream of N_2 at room temperature and 1 μL was injected for analysis. All derivatization methods were validated by analysis of ARA, DHA, and *Escherichia coli* whole cells.

Gas chromatography/mass spectrometry

Fatty acid methyl and ethyl ester derivatives were analyzed using a Varian Saturn 3 GC/MS system equipped with a ZB-5 ms capillary column 30 m×0.25 mm i.d., 0.25 μm film (Phenomenex USA, Torrance, CA, USA). The temperature program was 130°C to 170°C at 4°C/min, 170°C to 215°C at 2.7°C/min, 215°C for 3.34 min, with a total analysis time of 30 min. Carrier gas head-pressure was set to give a flow rate of 1 mL/min, with a 50:1 split. The injector and transfer line were maintained at 240°C and the manifold temperature was 210°C. Ionization was accomplished by electron impact (EI) at 70 eV, with a 3-min filament delay. Spectra were generated from full scans m/z 50 to 650, at a scan rate of one analytical scan per second and the background mass was set at m/z 49. The GC/MS method was optimized to provide peak resolution for FAMEs from the GLC-411 standard.

Fatty acid picolinyl ester derivatives were analyzed on the same instrument with the following temperature program: 150°C for 4 min, 150°C to 280°C at 20°C/min, 280°C for 19.5 min with a total analysis time of 30 min. All other parameters were as described above except that the filament delay was 10 min, and spectra were generated from full scans from m/z 50 to 500.

Chemical ionization (CI) experiments were conducted on the same instrument using the FAME GC/MS program, except the manifold temperature was reduced to 160°C. The MS parameters were as follows: selected-ejection chemical ionization (SECI) mode with acetonitrile as the reagent gas, 100 μs automatic-reaction control time, 1,000 μs ionization time, 128 ms reaction time, m/z 15

ionization storage level, 7.5 V_{0-p} reagent gas ion ejection amplitude, m/z 37.0 CI reaction storage level. Spectra were generated by full scans from m/z 80 to 650. All chromatograms were analyzed using the Wsearch32 2005 Software (version 1.6.2005; Melbourne, Australia).

Quantification of FAMEs (Conc.$_{FAME}$) was performed by comparing the area counts of the various fatty acid species (Area$_{FAME}$) with that of the internal standard, anthracene (Area$_{IS}$), Eq. (1):

$$\text{Conc.}_{FAME} = \frac{\text{Area}_{FAME} \times \text{Conc.}_{IS}}{\text{Area}_{IS}} \qquad (1)$$

The calculated Conc.$_{FAME}$ value is then divided by the dry cell weight (DCW) to obtain a concentration of FAME species normalized to the starting concentration of cells. The distribution of FAMEs per *C. thermocellum* strain was determined by dividing area counts for each FAME species by the total observed FAME area count, Eq. (2):

$$\%\text{FAME} = \frac{\text{Area}_{FAME}}{\sum \text{FAME}_{Area}} \times 100 \qquad (2)$$

The above equation was multiplied by 100 to give the product as the percent of each FAME species per *C. thermocellum* strain.

Statistical analysis for comparison of fatty acids between the two strains employed the paired *t* test. Comparisons were limited to equivalent fatty acids between the two species, i.e. wild-type (WT) *n*−14:0 vs. ethanol-adapted (EA) *n*−14:0. If $t_{calc} > t_{table}$ ($p < 0.05$, two-tailed), then the null hypothesis was rejected, and there was a significant difference between the means of the two fatty acid species (Table 1).

DPH labeling of whole cells and anisotropy

The anisotropy method was adapted from a previously described procedure (Bothun 2001). Approximately 15 mg of concentrated whole cells was washed with three 1 mL aliquots of 50 mM Tris–HCl (pH 7.5) by centrifugation (16,100×g, 5 min, 25°C) and the supernatants were discarded. After the final washing, the cells were resuspended in 1.5 mL of 50 mM Tris (pH 7.5), and 100 μL 0.1 mM DPH in THF solution was added. The mixture was incubated at 65°C for 1 h and then at 4°C overnight. The cells were then centrifuged (16,100×g, 5 min, 25°C), and the supernatant was discarded to remove any residual DPH. The pellet was resuspended in 10 mL of 50 mM Tris (pH 7.5) or the same buffer containing 5% (*w/v*) ethanol.

The fluorescence anisotropy of DPH-labeled cells was measured with a Varian Cary Eclipse fluorescence spectrophotometer (Walnut Creek, CA, USA), equipped with a

Table 1 Fatty acid composition and distribution of *C. thermocellum* wild-type (WT) and ethanol-adapted (EA) cells

Species (structure)[a]	FAME (%)[b,c]		Percent of WT[d]
	WT	EA	
13-Methyl-tridecanoic acid (*i*−14:0)	1.056±0.35	0.465±0.10	44.04*
Tetradecanoic acid (*n*−14:0)	1.385±0.37	0.652±0.23	47.09*
Plasmalogen *i*−14:0 (P *i*−14:0)	1.105±0.30	0.604±0.26	54.69*
Plasmalogen *n*−14:0 (P *n*−14:0)	1.293±0.33	0.658±0.19	50.88*
Plasmalogen 15:0 (P 15:0)	1.106±0.40	1.000±0.18	90.43
14-Methyl-pentadecanoic acid (*i*−16:0)	28.212±1.86	20.985±1.28	74.38*
Hexadecanoic acid (*n*−16:0)	21.768±0.57	16.218±1.19	74.51*
Plasmalogen *i*−16:0 (P *i*−16:0)	14.535±0.45	18.747±3.52	128.98
Plasmalogen *n*−16:0 (P *n*−16:0)	9.935±0.44	13.464±1.21	135.53*
15-Methyl-hexadecanoic acid (*i*−17:0)	4.426±0.36	7.608±0.86	171.91*
Heptadecanoic acid (*n*−17:0)	2.933±0.62	2.982±0.49	101.68
Plasmalogen *i*−17:0 (P *i*−17:0)	1.508±0.26	2.220±0.49	147.17
Plasmalogen *n*−17:0 (P *n*−17:0)	1.189±0.20	1.454±0.29	122.36
16-Methyl-heptadecanoic acid (*i*−18:0)	7.380±2.19	9.418±0.38	127.62
Octadecanoic acid (*n*−18:0)	2.170±0.53	3.523±0.74	162.40

i− iso-branching, *n*− normal or straight chain

*$p \leq 0.05$, statistically significantly different ($n=4$)

[a] Number of carbons:degree of unsaturation

[b] Comparisons made on percent FAME basis due to differences in micrograms per milligram DCW between WT and EA

[c] Values are averages of four replicates ±SEM

[d] Values represent change in EA relative to WT cells

custom view cell (Thar Technologies, Pittsburg, PA, USA) and manual polarizer accessory (part no. 00-100761-00) for both excitation (350 nm, slit width of 5 nm) and emission (452 nm, slit width of 10 nm; Bothun et al. 2005). The source was a Xenon pulse lamp (200–900 nm operating wavelength range with ±1.5 nm accuracy and ±0.2 nm reproducibility), and 1-s average sampling time was employed. Temperature of the view cell was modulated with heating tape and an Omega controller (model CN9000A). Each sample was heated from 24°C to 70°C with five readings taken every 2°C over the temperature ramp cycle. These five readings were averaged together to represent the average anisotropy ($<r>$) for the corresponding temperature. The reported data are the average and relative standard deviation from the average of three analytical replicate samples. The anisotropy (r) was calculated using Eq. (3):

$$r = \frac{(I_{VV} - gI_{VH})}{(I_{VV} + 2gI_{VH})} \qquad (3)$$

where I_{VV} is the intensity when excitation and emission are polarized vertical, I_{VH} is the intensity when excitation is polarized vertical and emission is polarized horizontal, and g is the grating factor.

The grating factor (g) was determined for each sample prior to heating Eq. (4):

$$g = \frac{I_{HV}}{I_{HH}} \qquad (4)$$

where I_{HV} is the intensity when excitation is polarized horizontal and emission is polarized vertical, and I_{HH} is the intensity when excitation and emission are polarized

horizontal. Essentially, the g factor is a correction for the monochromator transmission efficiency (Yun et al. 1993).

Results

Fatty acid structural determination

Earlier *C. thermocellum* studies used analytical approaches with limited capabilities. To enhance these previous studies, we used mass spectrometry to identify and quantify membrane lipids. However, since EI spectra of fatty acid methyl esters show extensive fragmentation and are not conducive to specific structural identities (Hamilton and Christie 2000), alternative methods of derivatization were evaluated. Picolinyl transesterification provides a simple method and mild reaction conditions that reduce the risk of fatty acid degradation. The nature of the picolinyl ester resulted in charge remote fragmentation products, allowing structure elucidation of the fatty acid alkyl chains (Fig. 1).

Picolinyl fragmentation of straight-chain fatty acids provided a repeating pattern of $[M]^+$–$(CH_2)_n$ mass units, after the loss of the terminal methyl group. Branched-chain fatty acids had a similar repeating pattern, but the $[M]^+$–$(CH_2)_n$ mass peak was absent at the branch point (Harvey 1982; Harvey 1992). The picolinyl ester of 14-methyl-pentadecanoic acid (the *iso*-methyl branched version of palmitic acid) is shown in Fig. 1a. For comparison, the mass spectrum of the picolinyl ester of palmitic acid is shown in Fig. 1b. The absence of an ion at m/z 318 in Fig. 1a was indicative of an *iso*-branch point in the molecule. In contrast, the mass spectrum in Fig. 1b showed

Fig. 1 Mass spectra of **a** picolinyl ester of 14-methyl-pentadecanoic acid and **b** picolinyl ester of palmitic acid. Straight-chain fatty acids provide a repeating pattern of [M-14]$^+$ mass units, with the exception of the terminal methyl group fragmentation [M-15]$^+$. The absence of m/z 318 due to the loss of 28 mass units from m/z 332 in **a** is indicative of an *iso*-branch point
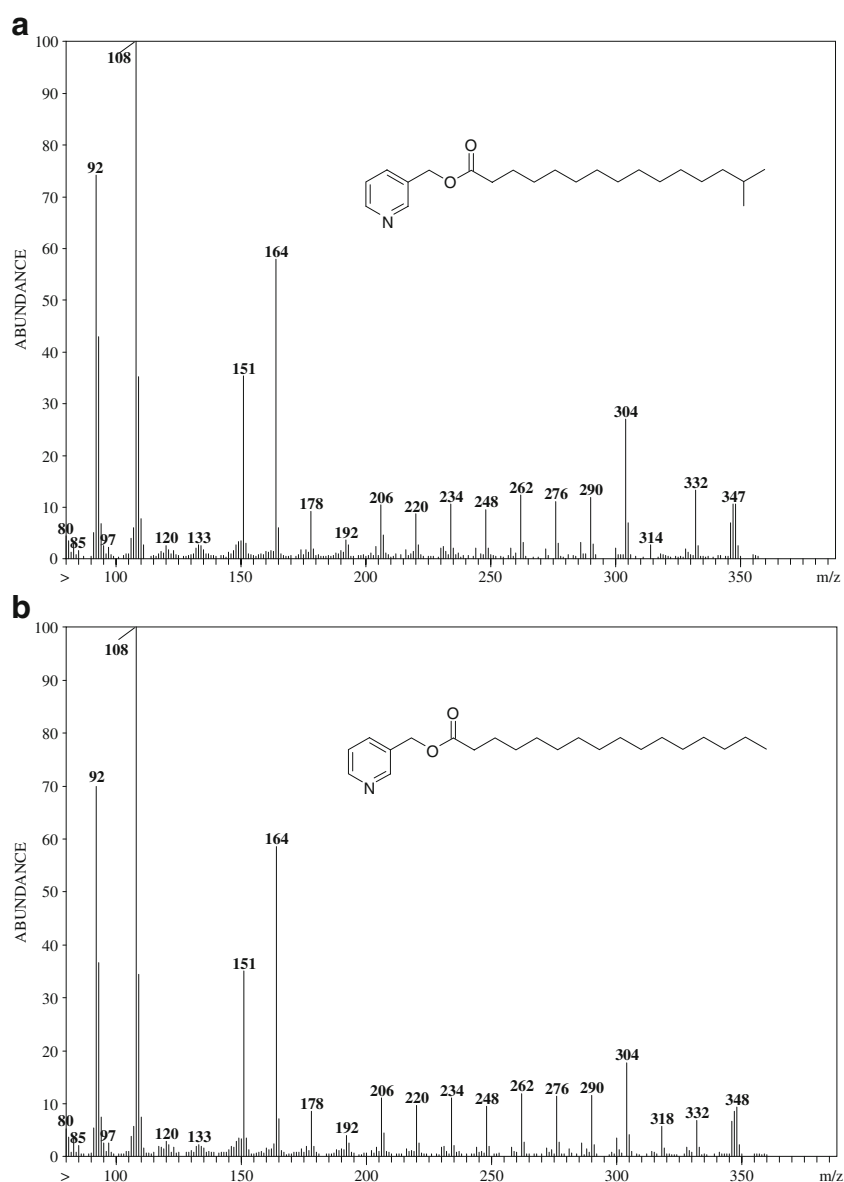

the loss of methylene groups from m/z 332 ([M-15]$^+$) to the McLafferty ion at m/z 151 indicative of the picolinyl ester of palmitic acid. This overall approach was used to identify the structures of fatty acids with other chain lengths (data not shown). Analysis of both *C. thermocellum* strains through picolinyl esterification yielded fatty acid structural profiles, consisting of *iso*- and normal-branched alkyl chains.

In addition to fatty acid moieties, ether-linked lipids, known as plasmalogens, were detected in both *C. thermocellum* strains. The plasmalogen vinyl-ether group forms an aldehyde, during the esterification reaction, which immediately converts to a dimethyl acetal. Unfortunately, the dimethyl acetals were not amenable to transesterification into picolinyl esters. Mass spectra generated with EI of these dimethyl acetals fail to provide a molecular ion, and

the only two prominent ions are m/z 255 representing loss of a methoxy group and m/z 75 loss of the dimethyl head group (Fig. 2a). An aldehyde, tridecanal, that reacted through the FAME procedure was used to synthesize a dimethyl acetal standard. The resulting tridecanal mass spectra exhibits a m/z 213 peak representing loss of a methoxy group and a m/z 75 again loss of the dimethyl head group (Fig. 2b). Comparison of EI generated mass spectra published by Christie provided further support for the plasmalogen conversion to dimethyl acetal fragmentation pattern (Christie 2007).

In an attempt to verify plasmalogen structures, CI experiments were conducted using acetonitrile as a reagent gas (Brenna 2006; Lawrence and Brenna 2006; Michaud and Brenna 2006; Michaud et al. 2005). Mass spectra from dimethyl acetal hexadecan-1-al (P 16:0) and dimethyl acetal

Fig. 2 Mass spectra from EI experiments from **a** dimethyl acetal of hexadecan-1-al (P 16:0) and **b** dimethyl acetal of tridecanal. Ionization was accomplished by EI at 70 eV. Spectra were generated from full scans m/z 50 to 650, at a scan rate of one spectrum per second, and the background mass was set at m/z 49. The m/z 255 (**a**) and 213 ions (**b**) represent [M-31]$^+$; the dimethyl head group corresponds to the m/z 75 ion in both spectra
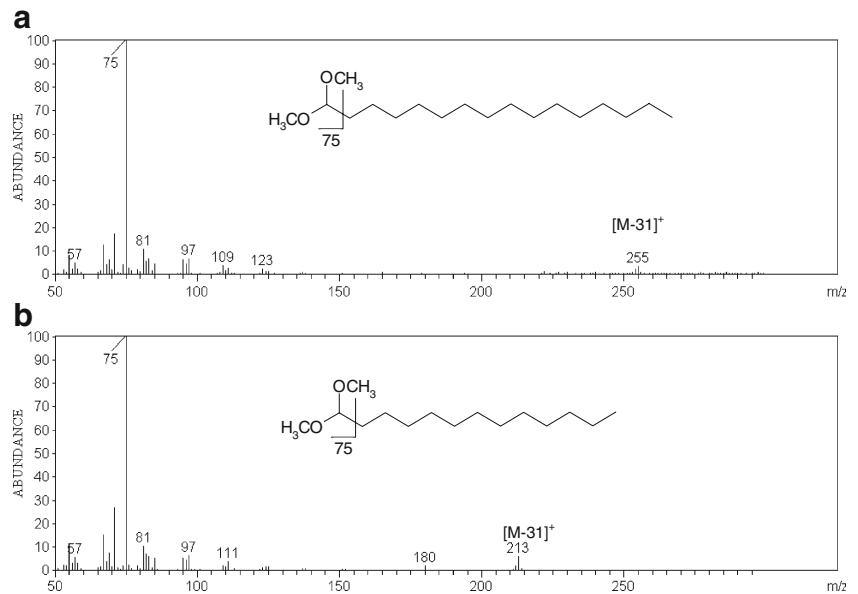
of tridecanal provide analogous fragmentation patterns (Fig. 3). Both spectra contain a minor [M-H]$^+$ peak, m/z 286 and 243, respectively, followed by loss of a methoxy group [M-30]$^+$, indicated by m/z 255 and 213. The dimethyl head group discussed above was not detected due to instrumental constants during chemical ionization.

Additional validation of dialkyl acetals was gained by substituting methanol with ethanol during the esterification reaction. The resulting EI mass spectra from diethyl acetal hexadecan-1-al (P 16:0) and diethyl acetal of tridecanal ions from the loss of ethoxy are 14 mass units greater than the dimethyl versions and loss of the diethyl head group, m/z 103, is 28 mass units greater than the dimethyl analog (Fig. 4).

Fatty acid profiles

Once structural identities were elucidated, quantitative fatty acid profiles of the WT and EA strains were determined. The total lipid content of WT and EA cells was approximately 82 and 56 μg per milligram DCW, respectively. The disparity in lipid content on a DCW basis was believed to be a result of variations in non-lipid components between the strains. This theory was supported by experiments that showed total carbohydrate levels in EA cells were five times greater than WT cells (data not shown). Since the recovered lipid contents (on a DCW basis) were different, the fatty acid profiles were compared on a percent area

Fig. 3 Mass spectra from CI experiments from **a** dimethyl acetal of hexadecan-1-al (P 16:0) and **b** dimethyl acetal of tridecanal. Ionization was accomplished by SECI mode with acetonitrile as the reagent gas. Spectra were generated from full scans m/z 85 to 650, at a scan rate of one spectrum per second, and the background mass was set at m/z 85. The m/z 286 (**a**) and 243 ions (**b**) represent [M-H]$^+$; loss of a methoxy group [M-30]$^+$ corresponds to m/z 286 and 213 ions, respectively
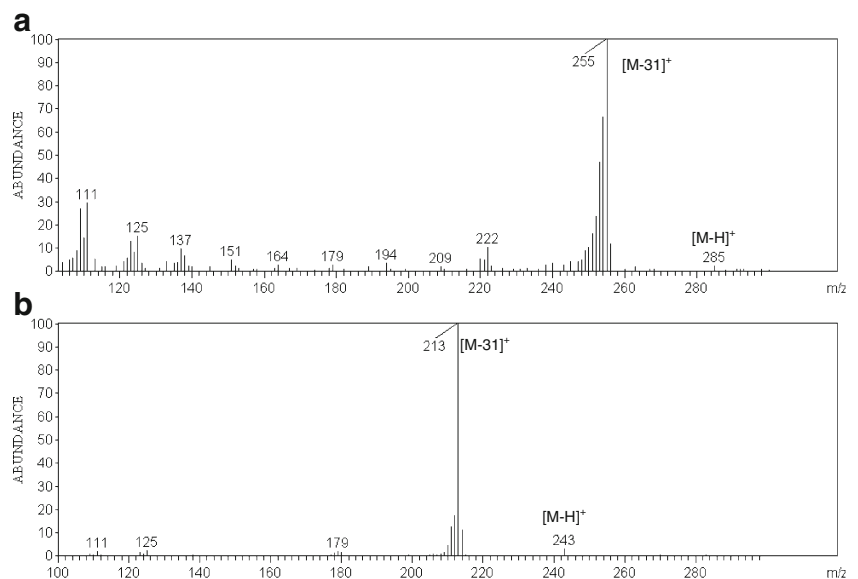
Fig. 4 Mass spectra from EI experiments from **a** diethyl acetal of hexadecan-1-al (P 16:0) and **b** diethyl acetal of tridecanal. Ionization was accomplished by EI at 70 eV. Spectra were generated from full scans m/z 50 to 650, at a scan rate of one spectrum per second, and the background mass was set at m/z 49. The m/z 269 (**a**) and 227 ions (**b**) represent $[M-45]^+$; the diethyl head group corresponds to the m/z 103 ion in both spectra
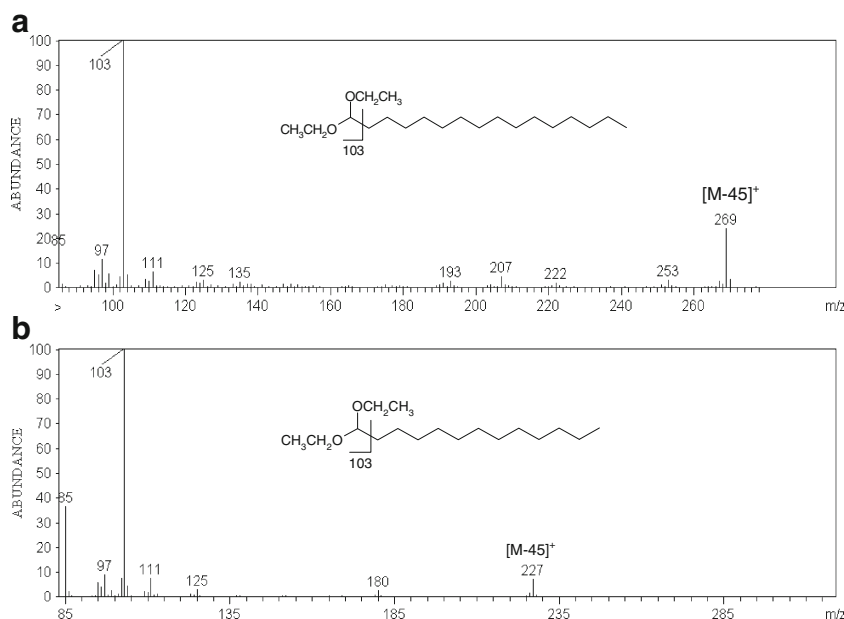
count basis (individual FAME area count divided by total FAME area count, Fig. 5).

Anisotropy measurements

Anisotropy was measured using whole cells incubated in buffer with either no ethanol present or 5% (w/v) exogenous ethanol. Membrane fluidity was assumed to be lowest at (24°C), and this arbitrarily corresponded to 100% anisotropy. Subsequent experimental values were reported as the percentage decrease in anisotropy (i.e., increase in fluidity) as a function of increasing temperature (Fig. 6). As the temperature was raised from 24°C to 70°C in the absence of ethanol, the anisotropy of WT cells decreased approximately 30% (Fig. 6). In contrast, there was only a 16% decrease in anisotropy for EA cells over the same temperature range
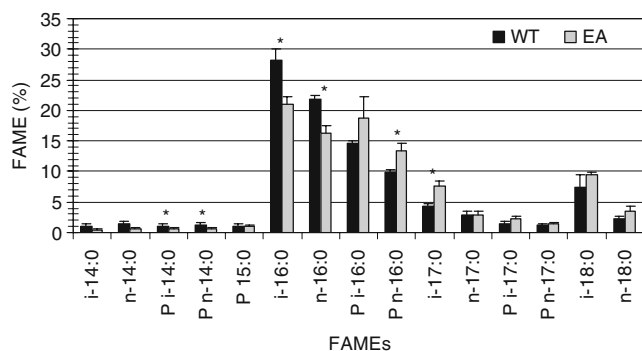
(Fig. 7). When 5% (w/v) ethanol was added to the buffer, WT and EA cells experienced 42% and 30% decreases in anisotropy, respectively (Fig. 7). In all experiments, the anisotropy changes were completely reversible when the temperature was decreased from 70°C to 24°C (data not shown).

The anisotropy experiments conducted without ethanol present allow a comparison of the two strains in an environment similar to WT batch culture. The EA cells have a higher average T_m, indicated by a lower change in anisotropy. In terms of fluidity, the higher T_m renders greater rigidity to the EA membrane in the absence of ethanol. The fatty acid data revealed that EA cells had a higher percentage of longer-chain fatty acids. This would result in the EA cells having a lower fluidity than WT cells when in similar environments (Tymczyszyn et al. 2005).
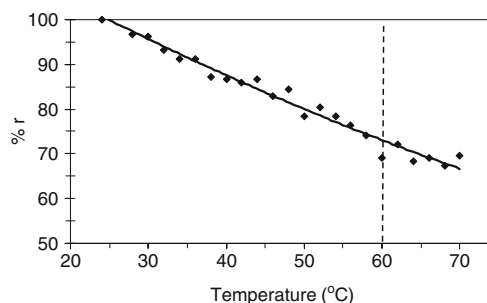

Fig. 5 Distribution of *C. thermocellum* fatty acids per WT and EA strains. Lipid extracts from dried cells were esterified with methanol to FAMEs then analyzed by GC/MS with anthracene as an internal standard. The error bars represent the standard error of the mean (SEM) from the averages of replicate reactions. Significant differences (*$p < 0.05$, $n=4$)

Fig. 6 Normalized steady-state fluorescence anisotropy with 0% (w/v) ethanol. *C. thermocellum* wild-type cells in 50 mM Tris (pH 7.5) as a function of temperature. Each data-point (*diamonds*) is the average of three analytical replicates; standard deviation error bars are concealed by the data-point symbols. Trendline fit to the data-points using a second order polynomial function. *Vertical dashed line* represents batch growth temperature
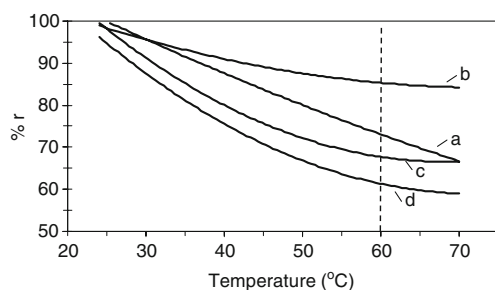
Fig. 7 Normalized steady-state fluorescence anisotropy effect of ethanol on fluidity comparison between *C. thermocellum* strains. *C. thermocellum* wild-type (**a**) and ethanol-adapted (**b**) in 50 mM Tris (pH 7.5) and wild-type (**c**) and ethanol-adapted (**d**) in 50 mM Tris (pH 7.5) with 5% (*w/v*) ethanol as a function of temperature. Data-points, omitted to reduce clutter, are the average of three analytical replicates; standard deviation error bars are concealed by the data-point symbols. Trendline fit to the data-points using a second order polynomial function. *Vertical dashed line* represents batch growth temperature

Discussion

A number of previous fermentation studies with *C. thermocellum* have focused efforts on improving ethanol production (Berberich et al. 2000; Bothun et al. 2005; Tailliez et al. 1989a, b). Studies concerned with changes to the fatty acid composition during ethanol adaptation, however, have been limited (Herrero et al. 1982). Herrero et al. found that an ethanol-adapted strain, C9, had a greater proportion of fatty acids with less than 14 carbons and more monounsaturated fatty acids. There also appeared to be an increase in *n-* and *anteiso*-branching, with a concurrent decrease in *iso*-branching (Herrero et al. 1982).

In the present study, we observed that adaptation to exogenous ethanol did not change the site of methyl branching or the index of unsaturation, as had been previously reported (Alexandre et al. 1994b; Herrero and Gomez 1980; Herrero et al. 1982). In fact, the present work found that the ratio of *iso-* to *n*-branched was higher in the EA strain for every fatty acid and plasmalogen, with the exception of 14:0 and P 14:0 (Table 2). Comparison of the WT and EA strains on a percentage basis revealed that WT had a greater percentage of fatty acids with chain lengths 16 carbons or less. On the other hand, the EA strain had a larger percentage of fatty acids and plasmalogens with chain lengths greater than 16 carbons (Fig. 5). This indicated that growth in 5% (*w/v*) ethanol increased the chain length of fatty acids incorporated into the membrane.

The presence of plasmalogen compounds was also detected as a component of the *C. thermocellum* membrane. The presence of plasmalogens was not surprising as these compounds have been found in other *Clostridia* species and are common for anaerobic bacteria (Johnston and Goldfine 1994; Johnston et al. 1994). Chemical ionization with acetonitrile has been used to elucidate double bond location

in the analysis of unsaturated fatty acids (Brenna 2006; Lawrence and Brenna 2006; Michaud and Brenna 2006; Michaud et al. 2005). The expectation was that CI could provide a "softer" method of ionization capable of producing structural characteristic ions. Chemical ionization did provide $[M-H]^+$ that fragmented to $[M-31]^+$, indicating that ions seen during EI were generated from the respective dimethyl acetal species. Data from the diethyl acetal fragmentation patterns corroborated spectra from both EI and CI of dimethyl acetals. The advantage to employing this three-tiered approach was that the chromatographic separation remains intact during each process, allowing peaks to be confidently identified based on mass spectra and retention times.

The absence of unsaturated fatty acids isolated from *C. thermocellum* in the present study raised concerns about the validity of the dervitization method. In order to confirm that unsaturated fatty acid methyl esters would have been observed from the saponification and FAME methods, reactions with ARA, DHA standards, and *E. coli* whole cells were conducted. Reactions with ARA and DHA yielded mass balance recoveries and FAME molecular ions of m/z 318 and 342, respectively. Qualitative analysis of the *E. coli* fatty acid profile was consistent with previously published data, which contained both unsaturated and cyclopropane fatty acids (Kurkiewicz et al. 2003). These experiments confirmed that the saponification and FAME procedures were applicable to sites of unsaturation (data not shown).

It is well established that microbes modify cell membrane composition in response to environmental stress (Evans et al. 1998; Ingram 1976; Jones 1989; Kropinski et al. 1987; Sinensky 1974). The concept of homeoviscous adaptation (i.e., membrane modifications that maintain an "optimal" degree of fluidity) has been supported by studies relating fatty acid profiles to solvent insult. The general model is that bacteria increase the number of unsaturated

Table 2 Fatty acid structural distribution of *C. thermocellum* wild-type (WT) and ethanol-adapted (EA)

Species[a]	WT[b]	EA[b]	Percent of WT[c]
14:0	0.76	0.71	93.4
P 14:0	0.85	0.92	108.2
16:0	1.30	1.29	99.2
P 16:0	1.46	1.39	95.2
17:0	1.51	2.55	168.9
P 17:0	1.27	1.53	120.5
18:0	3.35	2.67	79.7

P plasmalogen

[a] Number of carbons:degree of unsaturation

[b] Values represent the ratio of *i−* to *n−* isomers

[c] Values represent change in EA relative to WT cells

and short chain fatty acids in response to solvent insult. As a general rule, increasing the unsaturation index and decreasing the average fatty acid chain length both serve to increase fluidity of the membranes.

Previous studies conducted on the effect of exogenous solvents added to *C. thermocellum* batch cultures found that solvents impact bacterial proliferation and metabolism (Berberich et al. 2000). Growth inhibition caused by solvents dispersed in culture media is known as molecular toxicity (Berberich et al. 2000; Bothun et al. 2005); such toxicity is the result of interactions between the solvent and the membrane or membrane components. This solvent interaction disrupts membrane integrity by causing loss of protein function and increased membrane fluidity. Molecular toxicity is theorized to be responsible for growth inhibition of *C. thermocellum* WT cells at low ethanol concentrations (Berberich et al. 2000). Based on this theory, ethanol-adapted strains of *C. thermocellum* are believed to change their membrane composition in order to counter-act the effects of molecular toxicity.

In order to gain a more direct understanding of the relationship between fatty acid profiles and membrane fluidity, steady-state fluorescence anisotropy experiments were conducted as part of this study. Anisotropy is a measure of probe rotation by comparing the ratio of fluorescent emission in parallel and perpendicular polarizations. Within the context of this study, anisotropy correlates to the order of the fatty acid alkyl chains which is inversely related to fluidity, thus as the anisotropy value decreases, the fluidity of the membrane increases (Aricha et al. 2004). The rotation of DPH is a function of the fatty acid phase transition temperature, T_m. Longer saturated-chain fatty acids have a higher T_m due to a greater number of van der Waals interactions between acyl chains. Unsaturated fatty acids have lower transition temperatures than saturated fatty acids of similar length due to reduced van der Waals interactions as a result of the distorted geometry around the double bond (Morein et al. 1996). Below the T_m, the alkyl chains are in an ordered state and rotation of the DPH probe is restricted. With increasing temperature, the alkyl chains become disordered, allowing rotation of DPH. Rotation of DPH lowers the ratio of horizontal and vertical intensities, translating to a lower anisotropy (Alexandre et al. 1994a). Above the T_m of fatty acids, a phase transition occurs, which is reflected by a sudden increase in membrane fluidity (Shinitzky and Barenholz 1978). Because DPH integrates non-discriminately between acyl chains, a decrease in anisotropy represents an increase in the average fluidity of the membrane (Shinitzky and Barenholz 1978).

Anisotropy experiments with exogenous ethanol provided proof of the membrane fluidizing effects of ethanol (Kikukawa et al. 1997). The increased fluidity afforded by ethanol reduced the membrane rigidity for WT cells below

an optimum level. This sub-optimum membrane rigidity occurred because WT cells had a higher percentage of shorter chain fatty acids. Increased fluidity is believed to result in growth inhibition due to molecular toxicity of ethanol. The EA cells had a higher percentage of longer-chain fatty acids. Therefore, interaction between ethanol and the EA membrane increased the fluidity to a level that was consistent to that of WT cells without ethanol.

Since the plasmalogen concentration of *C. thermocellum* WT and EA membranes were 28% and 37%, respectively, their contribution to membrane structure and fluidity could be significant, as the vinyl-ether bond imparts different characteristics to the phosphotidyl group than the traditional fatty acid ester bond. Studies with plasmalogen membranes found that the T_m was lowered by 4–5°C (Nagan and Zoeller 2001). The plasmalogens' role might be to modify the T_m of the membrane in a similar manner as unsaturated fatty acids. Regulating membrane fluidity by means of plasmalogens might provide the cell with a more discrete mechanism of changing membrane properties.

The cell membrane functions as a protective barrier and serves a vital role in energy generating pathways, and so regulation of membrane integrity is essential for microbial survival and growth (Konings et al. 2002). The data from the fatty acid studies combined with the anisotropy data provide strong evidence for a refined model for acquired ethanol adaptation by *C. thermocellum* (Fig. 8). Adaptation was the result of changes to the fatty acid profile that increased rigidity, allowing the integrity of the membrane to be maintained during growth in the presence of ethanol (Chu-Ky et al. 2005). The data presented in this study supports the idea that EA cells maintain an optimum level of fluidity by increasing their fatty acid chain lengths in response to the increased fluidity provided by growth in media with ethanol.
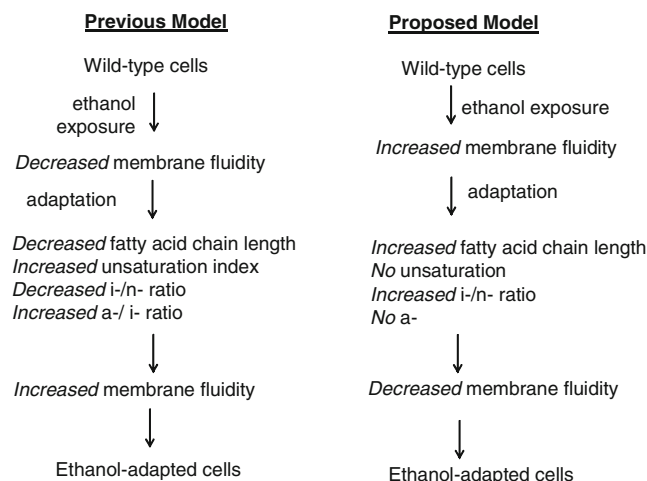

Fig. 8 Schematic of ethanol-adaptation mechanism. *i−* *iso*-branching, *n−* normal or straight chain, *a−* *anteiso*-branching

Mass spectrometry provided definitive identification of fatty acids present within the *C. thermocellum* membrane, and quantification of fatty acids and plasmalogens confirmed changes in cell membrane composition following ethanol treatment. The adaptation process resulted in a shift to longer-chain fatty acids, an increase in plasmalogen content, but did not increase the unsaturation index; these results were counter to previously published reports (Herrero et al. 1982). Anisotropy experiments corroborated the revised model of membrane adaptation and confirmed the fluidizing effect that ethanol has on both WT and EA membranes. Further support for the revised adaptation model was gained from EA anisotropy experiments without ethanol. In the absence of ethanol, the EA cells innately have higher membrane rigidity. Our results indicate that adaptation resulted from increased membrane rigidity.

Understanding the mechanism of membrane adaptation by *C. thermocellum* to acquire ethanol adaptation could be utilized to develop cultures that exhibit resistance to higher concentrations of ethanol. This in turn could lead to more cost-effective ethanol production and a step closer to consolidated bioprocessing.

References

Alexandre H, Berlot JP, Charpentier C (1994a) Effect of ethanol on membrane fluidity of protoplasts from saccharomyces-cerevisiae and kloeckera-apiculata grown with or without ethanol, measured by fluorescence anisotropy. Biotechnol Tech 8(5):295–300

Alexandre H, Rousseaux I, Charpentier C (1994b) Relationship between ethanol tolerance, lipid-composition and plasma-membrane fluidity in saccharomyces-cerevisiae and kloeckera-apiculata. FEMS Microbiol Lett 124(1):17–22

Aricha B, Fishov I, Cohen Z, Sikron N, Pesakhov S, Khozin-Goldberg I, Dagan R, Porat N (2004) Differences in membrane fluidity and fatty acid composition between phenotypic variants of Streptococcus pneumoniae. J Bacteriol 186(14):4638–4644

Berberich JA, Knutson BL, Strobel HJ, Tarhan S, Nokes SE, Dawson KA (2000) Product selectivity shifts in Clostridium thermocellum in the presence of compressed solvents. Ind Eng Chem Res 39(12):4500–4505

Bothun GD. (2001) Thesis (M.S. Ch. E.) University of Kentucky. Thesis (M.S. Ch. E.) University of Kentucky

Bothun GD, Knutson BL, Strobel HJ, Nokes SE (2005) Liposome fluidization and melting point depression by pressurized CO2 determined by fluorescence anisotropy. Langmuir 21(2):530–536

Brenna JT. (2006) Structural analysis of unsaturated fatty acid methyl ester isomers with acetonitrile covalent-adduct chemical ionization (CACI) tandem mass spectrometry. Lipid analysis and lipidomics : new techniques and applications. 157–172

Christie WW. (2007) The Lipid Library. http://www.lipidlibrary.co.uk/ (accessed 2007)

Chu-Ky S, Tourdot-Marechal R, Marechal P-A, Guzzo J (2005) Combined cold, acid, ethanol shocks in Oenococcus oeni: Effects on membrane fluidity and cell viability. Biochimica et Biophysica Acta (BBA)—Biomembranes 1717(2):118–124

Destaillats F, Angers P (2002) One-step methodology for the synthesis of FA picolinyl esters from intact lipids. J Am Oil Chem Soc 79 (3):253–256

Evans RI, McClure PJ, Gould GW, Russell NJ (1998) The effect of growth temperature on the phospholipid and fatty acyl compositions of non-proteolytic Clostridium botulinum. Int J Food Microbiol 40(3):159–167

Hamilton JTG, Christie WW (2000) Mechanisms for ion formation during the electron impact-mass spectrometry of picolinyl ester and 4, 4-dimethyloxazoline derivatives of fatty acids. Chem Phys Lipids 105(1):93–104

Harvey DJ (1982) Picolinyl esters as derivatives for the structural determination of long-chain branched and unsaturated fatty-acids. Biomed Mass Spectrom 9(1):33–38

Harvey DJ (1992) Mass spectrometry of picolinyl esters and other nitrogen-containing derivatives of lipids. Adv Lipid Res 1:19–80

Herrero AA, Gomez RF (1980) Development of ethanol tolerance in Clostridium thermocellum: effect of growth temperature. Appl Environ Microbiol 40(3):571–577

Herrero AA, Gomez RF, Roberts MF (1982) Ethanol-induced changes in the membrane lipid composition of Clostridium thermocellum. Biochim Biophys Acta 693(1):195–204

Ingram LO (1976) Adaptation of membrane lipids to alcohols. J Bacteriol 125(2):670–678

Ingram LO (1990) Ethanol tolerance in bacteria. Crit Rev Biotechnol 9(4):305–319

Jones RP (1989) Biological principles for the effects of ethanol. Enzyme Microb Technol 11(3):130–153

Johnston NC, Goldfine H (1994) Isolation and characterization of new phosphatidylglycerol acetals of plasmalogens: A family of ether lipids in clostridia. Eur J Biochem 223(3):957–963

Johnston NC, Goldfine H, Fischer W (1994) Novel polar lipid-composition of clostridium-innocuum as the basis for an assessment of its taxonomic status. Microbiology-Uk 140:105–111

Kikukawa T, Araiso T, Shimozawa T, Mukasa K, Kamo N (1997) Restricted motion of photoexcited bacteriorhodopsin in purple membrane containing ethanol. Biophys J 73(1):357–366

Konings WN, Albers SV, Koning S, Driessen AJM (2002) The cell membrane plays a crucial role in survival of bacteria and archaea in extreme environments. Antonie Van Leeuwenhoek International Journal of General and Molecular Microbiology 81(1–4):61–72

Kropinski AMB, Lewis V, Berry D (1987) Effect of growth temperature on the lipids, outer-membrane proteins, and lipo-polysaccharides of Pseudomonas-Aeruginosa Pao. J Bacteriol 169(5):1960–1966

Kurkiewicz S, Dzierzewicz Z, Wilczok T, Dworzanski JP (2003) GC/MS determination of fatty acid picolinyl esters by direct Curie-point pyrolysis of whole bacterial cells. J Am Soc Mass Spectrom 14(1):58

Lawrence P, Brenna JT (2006) Acetonitrile covalent adduct chemical ionization mass spectrometry for double bond localization in non-methylene-interrupted polyene fatty acid methyl esters. Anal Chem 78(4):1312–17

Lepage G, Roy CC (1988) Specific methylation of plasma nonesterified fatty acids in a one-step reaction. J Lipid Res 29 (2):227–35

Lynd LR, et al (2002) Microbial cellulose utilization: Fundamentals and biotechnology. Microbiol Mol Biol Rev 66(3):506–+

Michaud AL, Brenna JT (2006) Structural characterization of conjugated linoleic acid methyl esters with acetonitrile chemical ionization tandem mass spectrometry. Advances in Conjugated Linoleic Acid Research 3:119–138

Michaud AL, Lawrence P, Adlof R, Brenna J Thomas (2005) On the formation of conjugated linoleic acid diagnostic ions with acetonitrile chemical ionization tandem mass spectrometry. Rapid Commun Mass Spectrom 19(3):363–368

Morein S, Andersson A-S, Rilfors L, Lindblom G (1996) Wild-type Escherichia coli cells regulate the membrane lipid composition in a "window" between gel and non-lamellar structures. J Biol Chem 271(12):6801–6809

Nagan N, Zoeller RA (2001) Plasmalogens: biosynthesis and functions. Prog Lipid Res 40(3):199–229

Rani KS, Swamy MV, Sunitha D, Haritha D, Seenayya G (1996) Improved ethanol tolerance and production in strains of Clostridium thermocellum. World J Microbiol Biotechnol 12(1):57–60

Shinitzky M, Barenholz Y (1978) Fluidity parameters of lipid regions determined by fluorescence polarization. Biochim Biophys Acta 515(4):367–394

Sinensky M (1974) Homeoviscous adaptation— homeostatic process that regulates viscosity of membrane lipids in Escherichia-coli. Proc Natl Acad Sci U S A 71(2):522–525

Tailliez P, et al (1989a) Cellulose fermentation by an asporogenous mutant and an ethanol-tolerant mutant of clostridium-thermocellum. Appl Environ Microbiol 55(1):203–206

Tailliez P, et al (1989b) Enhanced cellulose fermentation by an asporogenous and ethanol-tolerant mutant of clostridium-thermocellum. Appl Environ Microbiol 55(1):207–211

Tymczyszyn EE, Gomez-Zavaglia A, Disalvo EA (2005) Influence of the growth at high osmolality on the lipid composition, water permeability and osmotic response of Lactobacillus bulgaricus. Arch Biochem Biophys 443(1–2):66–73

Weber FJ, de Bont JAM (1996) Adaptation mechanisms of microorganisms to the toxic effects of organic solvents on membranes. Biochim Biophys Acta (BBA)— Rev Biomembr 1286(3):225–245

Williams TI, Combs JC, Lynn BC, Strobel HJ (2007) Proteomic profile changes in membranes of ethanol-tolerant Clostridium thermocellum. Appl Microbiol Biotechnol 74(2):422–432

Yun I, Yang MS, Kim IS, Kang JS (1993) Bulk Vs transbilayer effects of ethanol on the fluidity of the plasma-membrane vesicles of cultured Chinese-hamster ovary cells. Asia Pac J Pharm 8(1):9–16